Libertas Academica
FREEDOM TO RESEARCH

Open Access: Full open access to this and thousands of other papers at http://www.la-press.com.

Particle Physics Insights

Electroweak Radiative Corrections to h^0 Production in Association with a Pair of Tau-sneutrino at $e^+ e^-$ Linear Colliders

B.Y. Al-Negashi[1,2], T.A. El-Azim[3] and I.A.M. Abdul-Magead[3]

[1]Department of Physics, Faculty of Science, Ain-Shams University, Cairo, Egypt. [2]Department of Physics, Faculty of Science, Taiz University, Taizz, Yemen. [3]Department of Physics, Faculty of Science, Cairo University, Giza, Egypt.

ABSTRACT: We study the production of the lightest neutral Higgs boson via the $e^+e^- \to \tilde{\nu}_\tau \bar{\tilde{\nu}}_\tau h^0$ process in the framework of the minimal supersymmetric standard model (MSSM). The aim of the study is first to calculate the full virtual one-loop electroweak (EW) corrections to the production of the $e^+e^- \to \tilde{\nu}_\tau \bar{\tilde{\nu}}_\tau h^0$ channel, and second to study the dependence of the lowest order, σ_0, and the full virtual one-loop radiative-corrected cross-section, σ, on the center of mass energy, $\sqrt{s}$, and the other model parameters. The study is done at the a typical minimal SUperGRAvity (mSUGRA) points (SPS 1b scenario) with relatively high Higgs vacuum expectation value (VEV), tan β, and with large value of tan β (SPS 4 scenario), which are defined in the supersymmetry parameter analysis (SPA) project. Our numerical results show that the radiative corrections are always positive in our chosen parameter spaces. The relative correction, $\Delta\sigma/\sigma_0$, varies in the ranges of [33%, 123%] and [63%, 71%] for SPS 1b and SPS 4 scenarios, respectively. The numerical results show that the best cross-section value and the EW relative corrections for the $e^+e^- \to \tilde{\nu}_\tau \bar{\tilde{\nu}}_\tau h^0$ channel are in favor of the SPS 1b scenario, and these corrections are so remarkable and they must be taken into account in precision measurements at future e^+e^- linear colliders.

PACS NO.: 12.15.-y, 13.66.-a, 13.85.Hd, 13.85.Lg

KEYWORDS: light neutral Higgs-boson particle, MSSM, tau-sneutrino particle

CITATION: Al-Negashi et al. Electroweak Radiative Corrections to h^0 Production in Association with a Pair of Tau-sneutrino at $e^+ e^-$ Linear Colliders. *Particle Physics Insights* 2015:7 1–12 doi:10.4137/PPI.S17559.

RECEIVED: June 2, 2014. **RESUBMITTED:** July 17, 2014. **ACCEPTED FOR PUBLICATION:** September 4, 2014.

ACADEMIC EDITOR: Hanna Moussa, Editor in Chief

TYPE: Original Research

FUNDING: Authors disclose no funding sources.

COMPETING INTERESTS: Authors disclose no potential conflicts of interest.

CORRESPONDENCE: bilquisyassen@yahoo.com

Paper subject to independent expert blind peer review by minimum of two reviewers. All editorial decisions made by independent academic editor. Upon submission manuscript was subject to anti-plagiarism scanning. Prior to publication all authors have given signed confirmation of agreement to article publication and compliance with all applicable ethical and legal requirements, including the accuracy of author and contributor information, disclosure of competing interests and funding sources, compliance with ethical requirements relating to human and animal study participants, and compliance with any copyright requirements of third parties. This journal is a member of the Committee on Publication Ethics (COPE).

1. Introduction

Uncovering the mechanism of symmetry breaking is one of the major tasks of the high energy colliders. The prime candidate is a Higgs mechanism, leading to the prediction of a physical scalar particle, the Higgs boson. The discovery or exclusion of the standard model (SM) Higgs boson is one of the primary scientific goals of the Large Hadron Collider (LHC) at European Organization for Nuclear Research (CERN). Indirect upper bound limit on the SM Higgs-boson mass of $m_h < 158$ GeV at 95% confidence level (CL) has been set using global fits to precision electroweak (EW) results.

Over the past 20 years, direct searches for the Higgs boson have been carried out at the Large Electron-Positron collider (LEP) collider, leading to a lower bound of $m_h > 114.4$ GeV at 95% CL[1] and at the Tevatron proton antiproton collider, excluding the mass range 162–166 GeV at 95% CL.[2] The success of the SM of Elementary Particle Physics has recently been confirmed by the observation of a state compatible with a (SM-like) Higgs boson at the LHC.[3]

In 2012, the proton–proton center of mass energy was increased to 8 TeV, and by the end of June, an additional integrated luminosity of more than 5 fb^{-1} was recorded by each of these experiments, thereby enhancing significantly the

sensitivity of the search for the Higgs boson. However, the complete profile of the Higgs boson can only be studied in the clean environment of e^+e^- collisions, such as at the future International Linear Collider (ILC).[4]

One of the most studied extensions of the SM is the minimal supersymmetric standard model (MSSM), which is expected to resolve theoretical difficulties existing in the SM.[5] The Higgs sector of the MSSM can be extended to contain two Charge Parity (CP)-even Higgs scalar bosons h^0 and H^0, one CP-odd Higgs boson A^0, and a charged Higgs pair $H^\pm$. The lightest neutral h^0 Higgs boson plays an important role in the extensions of the SM, the discovery of which in experiment will unequivocally imply the existence of physics beyond the SM.

The minimal SUperGRAvity (mSUGRA) model has become the most frequently used benchmark scenario for SUperSYmmetry (SUSY). The mSUGRA model has been widely used to analyze the expected SUSY particle spectrum and to compare the predictions to available and/or expected data from collider experiments.

There is a class of processes that is interesting for the studies of Higgs physics at linear collider called Higgs-boson production in association with a pair of final particles that can be pair-produced in e^+e^- collisions such as sneutrinos.[6–8] The LEP Collaboration results on the invisible width of the Z-boson show that the limit on the sneutrino mass is given as $m_{\tilde{\nu}} > 44.7$ GeV.

For the direct searches, the sneutrino mass limit is $m_{\tilde{\nu}} > 94$ GeV, with the assumption of mass degeneracy and the presence of only the left-handed sneutrinos, $\tilde{\nu}_l$.[9,10] The couplings of sparticles to Higgs bosons are of special importance since they probe the electroweak symmetry breaking (EWSB) sector and might decide which Higgs scenario is at work. The couplings of the h^0 boson to sfermion pairs, $g_{h\tilde{f}_i\tilde{f}_j}$, can be carried out by studying the $e^+e^- \to \tilde{\nu}_\tau\bar{\tilde{\nu}}_\tau h^0$ channel.

In this paper, we investigate the prospects of measuring the lightest neutral CP-even Higgs boson, h^0, coupling to a pair of tau-sneutrino, $\tilde{\nu}_\tau\bar{\tilde{\nu}}_\tau$, which can be best performed in the clean environment of future high energy e^+e^- colliders. Up to the small contribution of the diagrams where the h^0 boson is emitted from the Z-boson line, the cross-sections are directly proportional to the square of the $\tilde{\nu}_\tau\bar{\tilde{\nu}}_\tau h^0$ couplings, which would then be, in principle, measurable in this process.[11]

The production of the lightest neutral Higgs bosons in association with pairs of muon-sneutrino in the MSSM model at the electron–positron collider has been studied in Refs. 12 and 13 over the kinematically allowed range for each of the Born level and the full virtual one-loop EW corrections. We continue to study another operation that is $e^+e^- \to \tilde{\nu}_\tau\bar{\tilde{\nu}}_\tau h^0$ with the same strategy for the work. The shift of the parameters in the Snowmass point from SPS 1a to SPS 6[14] leads to a configuration in which the sneutrinos are heavier than the light chargino and next to the lightest neutralino. Therefore, using the same calculation strategy as in Ref. 15, we have adopted the reference points SPS 1b and SPS 4 that are defined in the supersymmetry parameter analysis (SPA) project for carrying out detailed analyses of our process at the future ILC.

The outline of this paper is as follows. In Section 2, the analytical calculations of the Born cross-section and the full one-loop EW corrections, including Quantum-Electro Dynamics theory (QED) contributions to the $e^+e^- \to \tilde{\nu}_\tau\bar{\tilde{\nu}}_\tau h^0$ process, are given. The calculation results and the scan over the MSSM parameter space are presented in Section 3. The conclusion is discussed in Section 4.

2. Calculations

2.1. Conventions and notations in analytical calculations. In the $e^+e^- \to \tilde{\nu}_\tau\bar{\tilde{\nu}}_\tau h^0$ channel, there are totally 21 tree-level Feynman diagrams that are shown in Figure 1.

The notations are defined as

$$e^+(p_1,\sigma_1)+e^-(p_2,\sigma_2)\to\tilde{\nu}_\tau(p_3)+\bar{\tilde{\nu}}_\tau(p_4)+h^0(p_5) \qquad (1)$$

where the four-momentum of the incoming positron and electron are p_1 and p_2, respectively. The four-momentum of outgoing tau-sneutrino, anti-tau-sneutrino, and h^0 boson are denoted as p_3, p_4, and p_5, respectively. All these momenta obey the on-shell (OS) equations $p_1^2 = p_2^2 = m_e^2$, $p_3^2 = p_4^2 = m_{\tilde{\nu}_\tau}^2$, and $p_5^2 = m_{h^0}^2$.

The helicities of the positron and electron are σ_i, which take the values $\sigma_i = \pm 1/2$, but we often use only the sign to indicate the helicity. This implies that the lowest-order and one-loop amplitudes vanish unless $\sigma_1 = -\sigma_2$. The electron mass is neglected whenever possible.

The total tree-level cross-section with unpolarized incoming particles is given by

$$\sigma_0(e^+e^-\to\tilde{\nu}_\tau\bar{\tilde{\nu}}_\tau h^0)=\frac{(2\pi)^4}{4\left|\vec{p}_1\right|\sqrt{s}}\int\overline{\sum_{\text{spin}}}\left|M_0\right|^2 d\Phi_3 \qquad (2)$$

The summation is taken over the spins of initial and final particles. The factor 1/4 is because of averaging over the polarization states of the electron and positron, and the bar over summation indicates averaging over initial spins. $d\Phi_3$ is the three-particle phase-space element defined as

$$d\Phi_3=\delta^{(4)}\left(p_1+p_2-\sum_{i=3}^{5}p_i\right)\prod_{j=3}^{5}\frac{d^3P_j}{(2\pi)^3E_j} \qquad (3)$$

2.2. One-loop *EW* corrections to the $e^+e^- \to \tilde{\nu}_\tau\bar{\tilde{\nu}}_\tau h^0$ process. In our *EW* correction calculation, we adopt the t'Hooft–Feynman gage and the same definitions of one-loop integral functions as in Ref. 16. We use the dimensional reduction (DR) regularization scheme, which is supersymmetric invariant at the one-loop level, to regularize ultraviolet (UV) divergences, and we also adopt the OS conditions to renormalize the relevant fields.[17] For the sfermion sector, the

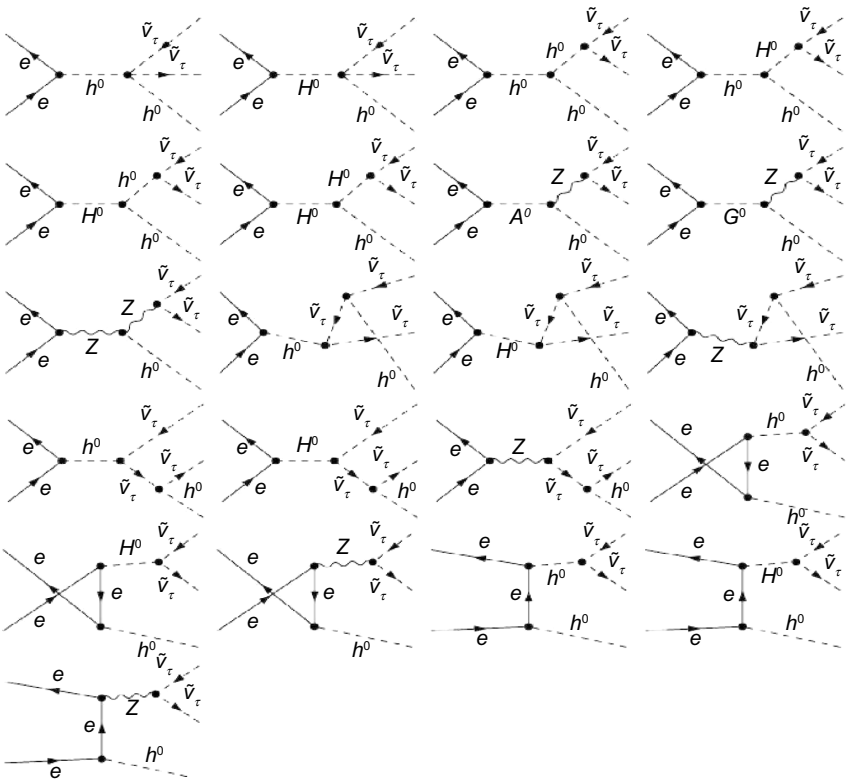

Figure 1. The lowest-order Feynman diagrams for the $e^+e^- \to \tilde{\nu}_\tau \bar{\tilde{\nu}}_\tau h^0$ process.

renormalization of constants for the mass matrices in the L, R basis for each sfermion species, $M^{\tilde{f}}$, and for the mass eigenstates $\tilde{f}^s$ ($s = 1, 2$ in general, $s = L$ for $f = v$) is carried out by means of the transformation

$$\begin{aligned} M^{\tilde{f}} &\to M^{\tilde{f}} + \delta M^{\tilde{f}} \\ \tilde{f}^s &\to \left(\delta_{st} + \tfrac{1}{2}\left[\delta Z^{\tilde{f}}\right]_{st}\right)\tilde{f}^t \end{aligned} \tag{4}$$

where $\delta M^{\tilde{f}}$ contains the counter terms for the parameters in the mass matrix $M^{\tilde{f}}$. The sneutrino mass matrix fields actually consist of only one single element. The general complex 2×2 matrices $\delta Z^{\tilde{f}}$ represent the field-renormalization constants. In the $f = v$ case, with a single field-renormalization constant, $\delta Z^{\tilde{v}} = \delta Z_L$.[18]

The (UV) divergences ($E \to \infty$) appearing from the one-loop diagrams are canceled by the contributions from the counter-term diagrams. The one-loop level virtual *EW* corrections to the cross-section are expressed as

$$\sigma_{\text{vir}}^{EW} = \frac{(2\pi)^4}{2\left|\overrightarrow{p_1}\right|\sqrt{s}} \int d\Phi_3 \sum_{\text{spin}} \text{Re}(M_0^\dagger M_{\text{vir}}^{EW}) \tag{5}$$

where $\overrightarrow{p_1}$ is the center of mass system (c.m.s.) three-momentum of the incoming positron. M_{vir}^{EW} is the renormalized total amplitude of all the one-loop *EW*-level Feynman diagrams, including self-energy, vertex, box, and counter-term diagrams.

Before discussing the QED corrections, it is worth mentioning that the full virtual radiative *EW*-corrected total cross-section involves both the Born contribution and the remaining set of one-loop corrections, which can be written as the sum of self-energies, vertex corrections, and box contributions.

Although the taking into account of the box virtual correction part leads to the improvement of the Born cross-section value, the Monte Carlo sampling of the box virtual correction part is very slow and takes a very long time to obtain the requested accuracy. Therefore, the constraint *no SUSY particles* is considered.

2.3. QED corrections. In calculating the correction from the real photon emission process,

$$e^+(p_1, \sigma_1) + e^-(p_2, \sigma_2) \to \tilde{v}_\tau(p_3) + \bar{\tilde{v}}_\tau(p_4) + h^0(p_5) + \gamma(k_\gamma, \lambda) \tag{6}$$

where k and γ denote the photon momentum and helicity; use is made of the MadGraph5 program[19] to generate the tree-level diagrams and amplitudes. The integration in four-body phase-space is carried out. One adopt the general phase-space slicing method to separate the soft-photon emission singularity from the real photon emission processes[20] and divide process into the cross-section of the real photon emission process into

$$\begin{aligned} \sigma_{real}^{EW} &= \sigma_{soft}^{EW} + \sigma_{hard}^{EW} \\ &= \sigma_0 \left(\delta_{soft}^{EW} + \delta_{hard}^{EW}\right) \end{aligned}$$

The soft part has radiated photon energy $k_\gamma^0 > \Delta E_\gamma$, and the hard part with radiated photon energy, $k_\gamma^0 > \Delta E_\gamma$, where $k_\gamma^0 = \sqrt{\left|\vec{k}_\gamma\right|^2 + m_\gamma^2}$ and m_γ is the photon mass.

Both $\delta_{\text{soft}}^{EW}$ and $\delta_{\text{hard}}^{EW}$ depend on the arbitrary soft cutoff $\Delta E/E_b$, where $E_b = \sqrt{s}/2$ is the electron beam energy in the c.m.s., but the total cross-section of the real photon emission process $\sigma_{\text{real}}^{EW}$ is cutoff independent.

During the calculation of the *EW* corrections to the real photon emission process, the infrared (IR) divergences ($E \to 0$) originating from the exchange of virtual massless photon correction are canceled out by the real photon bremsstrahlung correction in the soft-photon limit.[17,21] Therefore, the sum of the virtual and soft cross-sections is independent of the (IR) regulator m_γ. This is only valid if ΔE is small compared to all relevant energy scales.

The hard contribution is computed using the Monte Carlo technique, but it is not taken into account in this study. As explained above, QED correction can be isolated and studied separately.

3. Numerical Results and Discussion

As a calculation frame, the OS renormalization scheme has been chosen where all particle masses are defined as pole masses; ie, the particle masses are identified with the physical propagator poles and the OS physical fields are normalized to unity, as, eg, described in Ref. 16.

In the amplitude calculation of the $e^+e^- \to \tilde{\nu}_\tau \bar{\tilde{\nu}}_\tau h^0$ channel involving one-loop contributions, we create all the tree-level, one-loop Feynman diagrams and their relevant amplitudes in the t'Hooft–Feynman gage by using FeynArts-3.6.[22] This package uses algorithms that can deal with supersymmetric theories,[4] and the Feynman amplitudes are subsequently reduced by FormCalc-7.1[23] and then converted to a Fortran program. The LoopTools-2.7[24] is a package for evaluation of scalar and tensor one-loop integrals based on the ff package by G.J. van Oldenborgh.

All counter terms required for propagators and vertices appearing in the amplitudes have become part of the FeynArts-3.6[22] package for the MSSM. The phase-space integration for the $e^+e^- \to \tilde{\nu}_\tau \bar{\tilde{\nu}}_\tau h^0$ process is implemented by adopting 2 to 3.F subroutine in FormCalc-7.1 package.

3.1. Input parameters.

3.1.1. SM parameters. We use the set of SM parameters,[25] which coincides with the one used in Ref. 26.

3.1.2. MSSM parameters. The following are the free parameters that are used here:

- Higgs sector is parameterized by the mass m_{A^0} of the CP-odd neutral Higgs boson, A^0, and the ratio of the Higgs vacuum expectation value (VEV), tan β. For the other neutral Higgs masses, which receive significant radiative corrections, the two-loop approximation formulas are used.[27]
- Sfermions are characterized by a common soft-breaking sfermion mass $M_{\text{SUSY}} \equiv \tilde{M}_L = \tilde{M}_R$ and soft trilinear couplings, A_f, which determine the mixing in the sfermion families. The third family trilinear couplings are the most relevant ones, ie, $A_0 = A_t = A_b = A_\tau$.
- Charginos and neutralinos are fixed by choosing the higgsino mass term, μ, and a value for the gaugino mass terms at the *EW* scale.

This work is performed in the constrained MSSM or mSUGRA model[4] where the mSUGRA soft-breaking parameters obey a set of universal boundary conditions at the Grand Unification Theory (GUT) scale, $M_{\text{GUT}} = 2 \times 10^{16}$ GeV, so that the EW symmetry is broken radiatively. The mSUGRA scenario has only four continuous free parameters and an unknown sign in addition to the parameters of the SM:

$$\tan\beta, M_2, M_{\text{SUSY}}, A_0, \text{sign}(\mu)$$

where tan β is the ratio of the Higgs VEV, M_2 is the common soft–SUSY breaking gaugino mass, M_{SUSY} is a uniform scalar mass, A_0 is the scalar trilinear couplings, and μ is the Higgsino mass parameter, the absolute value of which is determined by the requirement of a proper EWSB. From these input values, one can evolve the Renormalization Group Equation (RGEs) down to the weak scale at which point the observable spectrum can be evaluated.

As a numerical demonstration, we generally adopt the following two benchmark scenarios SPS 1b and SPS 4, which are defined in the SPA project as follows[28]:

- *SPS 1: typical mSUGRA scenario*—This scenario consists of a typical mSUGRA point with an intermediate value of tan β and a model line attached to it (SPS 1a), and a typical mSUGRA point with relatively high tan β (SPS 1b). The two points lie in the bulk of the cosmological region.
- *SPS 4: mSUGRA scenario with large tan β*—The large value of tan β in this scenario has an important impact on the phenomenology in the Higgs sector.

Table 1. SM parameters.

MASSES		
$m_e = 0.51099$ MeV	$m_\mu = 105.65$ MeV	$m_\tau = 1777$ MeV
$m_u = 53.8$ MeV	$m_c = 1.50$ GeV	$m_t = 174.3$ GeV
$m_d = 53.8$ MeV	$m_s = 150$ MeV	$m_b = 4.25$ GeV
EW COUPLING PARAMETERS		
$\alpha_{EW}(m_Z) = 1/127.934$		
$\cos\theta_w = m_W/m_Z$, $\sin^2\theta_w = 1 - \cos^2\theta_w$		
$m_W = 80.4$ GeV, $m_Z = 91.1876$ GeV		

Table 2. The benchmark points of SPS 1b and SPS4 scenarios as defined in the SPA project.

	tan β	M_{SUSY}	M_2	A_0	SIGN(μ)
SPS 1b	30	200	400	0	+
SPS 4	50	400	300	0	+

The SPS 1b and SPS 4 points are given in Table 2. The relevant parameters of SPS 1b and SPS 4 points are listed in Table 3. These Snowmass Points and Slopes (SPS)[29] satisfy all the available high- and low-energy precision data, as well as the bounds for the masses of the SUSY particles and the bounds from cosmology.

3.2. Results. We have classified the numerical calculations into three groups according to benchmark points as follows. In Group I, we have adopted the typical mSUGRA benchmark points as depicted in Table 2. Group II studied the impact of the M_{SUSY} parameter on the $\tilde{\nu}_\tau\bar{\tilde{\nu}}_\tau h^0$ production while maintaining the rest of the benchmark points in Table 2 as they are without change. The effect of the tan β parameter of the $e^+e^- \to \tilde{\nu}_\tau\bar{\tilde{\nu}}_\tau h^0$ channel will be thoughtful via Group III. The work strategy to deal with the figures can be listed in Table 4.

3.2.1. Group I. In the numerical calculations of this group, we are dealing with exactly the benchmark points of SPS 1b and SPS4 scenarios as defined in the SPA project (Table 2).

Figure 2 illustrates the Born cross-section dependence on the c.m.s. energy, $\sqrt{s}$, of the polarized and the unpolarized beams of the $e^+e^- \to \tilde{\nu}_\tau\bar{\tilde{\nu}}_\tau h^0$ channel. For the two chosen scenarios SPS 1b (Fig. 2A) and SPS 4 (Fig. 2B), the polarized beam has the maximal value cross-section. However, the unpolarized beam is adopted in this work.

Figure 3 represents the Born and the full virtual radiative *EW*-corrected total cross-sections as well as the QED contributions at the SPS 1b and SPS 4 points, respectively. The tau-sneutrino and the lightest neutral Higgs-boson masses at the SPS 1b and SPS 4 points are fixed in the mSUGRA model by using FormCalc program with the input parameters as given in Table 3. For the SPS 1b and SPS 4 scenarios, it is clear that the corrected cross-sections are always more than the corresponding tree-level cross-sections; ie, the radiative corrections are always positive in our chosen parameter spaces. This is consistent with our numerical results in the corresponding reaction, $e^+e^- \to \tilde{\nu}_\mu\bar{\tilde{\nu}}_\mu h^0$, as in Ref. 12.

Figure 4 exhibits the relationship between the relative one-loop correction, $\Delta\sigma/\sigma_0$, of the $e^+e^- \to \tilde{\nu}_\tau\bar{\tilde{\nu}}_\tau h^0$ process

Table 3. Mass spectrum of supersymmetric particles and Higgs bosons of SPS 1b (left) and SPS 4 (right).

SCENARIOS							
SPS 1b				SPS 4			
PARTICLE	MASS/[GeV]	PARTICLE	MASS/[GeV]	PARTICLE	MASS/[GeV]	PARTICLE	MASS/[GeV]
h^0	114.7	$\tilde{X}_1^0$	162.2	h^0	112.5	$\tilde{X}_1^0$	120.5
H^0	524.7	$\tilde{X}_2^0$	306.2	H^0	329.0	$\tilde{X}_2^0$	225.6
A^0	524.6	$\tilde{X}_3^0$	517.5	A^0	329.0	$\tilde{X}_3^0$	398.1
$H^\pm$	531.1	$\tilde{X}_4^0$	530.6	$H^\pm$	339.9	$\tilde{X}_4^0$	413.6
$\tilde{g}$	936.4	$\tilde{\nu}_e$	329.1	$\tilde{g}$	732.9	$\tilde{\nu}_e$	441.8
$\tilde{X}_1^\pm$	306.2	$\tilde{\nu}_\mu$	329.0	$\tilde{X}_1^\pm$	225.4	$\tilde{\nu}_\mu$	441.6
$\tilde{X}_2^\pm$	530.9	$\tilde{\nu}_\tau$	318.2	$\tilde{X}_2^\pm$	414.2	$\tilde{\nu}_\tau$	386.6
$\tilde{e}_L$	338.7	$\tilde{e}_R$	253.8	$\tilde{e}_L$	449.2	$\tilde{e}_R$	417.3
$\tilde{\mu}_L$	338.8	$\tilde{\mu}_R$	253.7	$\tilde{\mu}_L$	449.1	$\tilde{\mu}_R$	416.9
$\tilde{\tau}_L$	197.2	$\tilde{\tau}_R$	345.4	$\tilde{\tau}_L$	259.4	$\tilde{\tau}_R$	414.1
$\tilde{u}_L$	874.5	$\tilde{u}_R$	845.4	$\tilde{u}_L$	761.9	$\tilde{u}_R$	744.7
$\tilde{d}_L$	878.0	$\tilde{d}_R$	843.3	$\tilde{d}_L$	765.9	$\tilde{d}_R$	744.0
$\tilde{c}_L$	874.5	$\tilde{c}_R$	845.4	$\tilde{c}_L$	761.9	$\tilde{c}_R$	744.7
$\tilde{s}_L$	878.0	$\tilde{s}_R$	843.3	$\tilde{s}_L$	765.9	$\tilde{s}_R$	744.0
$\tilde{t}_L$	659.1	$\tilde{t}_R$	836.0	$\tilde{t}_L$	543.9	$\tilde{t}_R$	693.0
$\tilde{b}_L$	771.4	$\tilde{b}_R$	822.1	$\tilde{b}_L$	611.5	$\tilde{b}_R$	680.3

Table 4. The strategy of the work.

SPS 1b			SPS 4		
Group I	Figure 2 – a Figure 3 – a Figure 4 – a Figure 5 – a	Table 2, exactly.	**Group I**	Figure 2 – b Figure 3 – b Figure 4 – b Figure 5 – b	Table 2, exactly.
Group II	Figure 6 – a Figure 7 – a Figure 8 – a Figure 9 – a Figure 10 – a	M_{SUSY} is of the range [200 GeV $\rightarrow$ 650 GeV], Table 2 gives the values of the other parameters.	**Group II**	Figure 6 – b Figure 7 – b Figure 8 – b Figure 9 – b Figure 10 – b	M_{SUSY} is of the range [400 GeV $\rightarrow$ 650 GeV], Table 2 gives the values of the other parameters.
Group III	Figure 11 – a Figure 12 – a Figure 13 – a Figure 14 – a Figure 15 – a	tan β is of the range [5 $\rightarrow$ 30], for the other parameters, Table 2.	**Group III**	Figure 11 – b Figure 12 – b Figure 13 – b Figure 14 – b Figure 15 – b	tan β is of the range [5 $\rightarrow$ 50], for the other parameters, Table 2.

and the colliding energy, $\sqrt{s}$. As $\sqrt{s}$ goes up, $\Delta\sigma/\sigma_0$ increases rapidly in the vicinity of threshold energy, $\tilde{\nu}_\tau\bar{\tilde{\nu}}_\tau h^0$, and then smoothly increases from 33% to 123% between the c.m.s energies 0.5 and 2.5 TeV (Fig. 4A). The corresponding relative one-loop correction is depicted in Figure 4B for the SPS 4 parameter space. The correction varies from 63% at the threshold energy 1 TeV to 71% at the 2.5 TeV. The relative correction, $\Delta\sigma/\sigma_0$, of the SPS 1b and SPS 4 scenarios are of order of 90% and 8%, respectively, while $\Delta\sigma/\sigma_0$ of the SPS 1b and SPS 4 parameter spaces of the corresponding reaction, $e^+e^- \rightarrow \tilde{\nu}_\mu\bar{\tilde{\nu}}_\mu h^0$, are of order of 83% and 13%, respectively.[12]

Figure 5 shows the percentage of the relative one-loop correction, $\Delta\sigma/\sigma_0$, as a function of μ parameter in each of SPS 1b and SPS 4 scenarios, for two different values of the colliding energy, $\sqrt{s} = 1.2$ TeV and $\sqrt{s} = 1.7$ TeV, respectively.

For the two chosen scenarios, the effect of μ parameter on the total cross-section as a function of the c.m.s energy at the values μ = 150, 200, and 250 GeV is rather minute at the Born approximation level and at the full virtual *EW*-corrected total cross-section. Similar results are obtained in Ref. 12 where the μ parameter in each of SPS 1b and SPS 4 scenarios in the same range, from 150 to 250 GeV, has a small effect on $\Delta\sigma/\sigma_0$.

3.2.2. Group II. In this group, one baptizes to change the M_{SUSY} parameter in Table 2 to study its effect on the $\tilde{\nu}_\tau\bar{\tilde{\nu}}_\tau h^0$ production while maintaining the rest of the parameters as they are in Table 2. Figure 6 shows the percentage of the relative one-loop correction, $\Delta\sigma/\sigma_0$, of the $e^+e^- \rightarrow \tilde{\nu}_\tau\bar{\tilde{\nu}}_\tau h^0$ process as a function of the c.m.s energy, $\sqrt{s}$.

Figures 7 and 8 represent the dependence of the tree-level cross-section, σ_0, on the tau-sneutrino, $m_{\tilde{\nu}_\tau}$, and the lightest

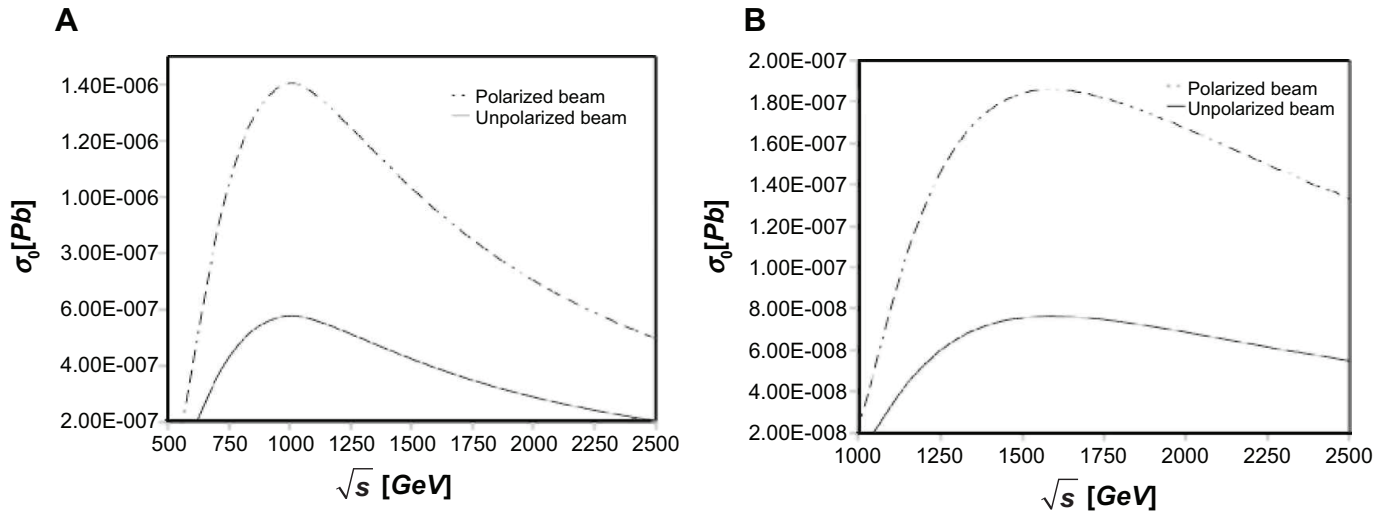

Figure 2. The Born cross-section for the $e^+e^- \rightarrow \tilde{\nu}_\tau\bar{\tilde{\nu}}_\tau h^0$ process as a function of the colliding energy, $\sqrt{s}$, for the polarized and unpolarized beams.

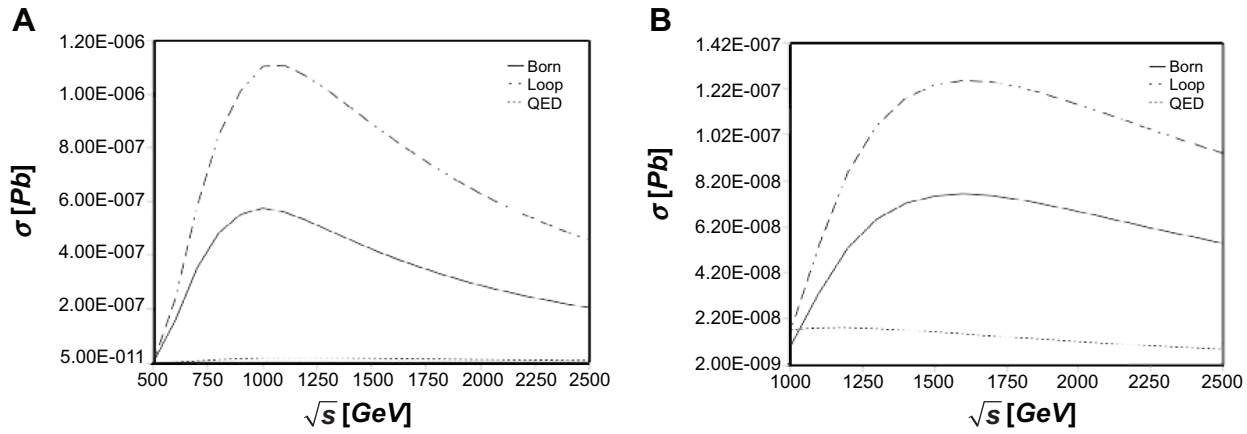

Figure 3. The Born cross-section, σ_0, the full virtual *EW*-corrected total cross-section, σ, and QED contributions as function of the colliding energy, $\sqrt{s}$, for the unpolarized beam at $\mu = 250$ GeV.

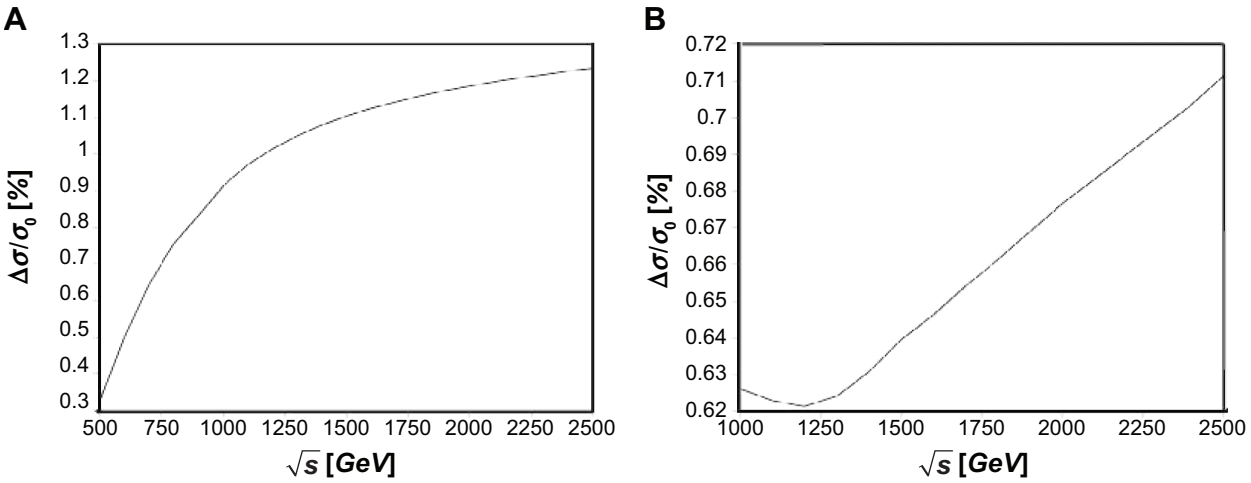

Figure 4. $\Delta\sigma/\sigma_0$ as a function of $\sqrt{s}, (\Delta\sigma = \sigma - \sigma_0)$.

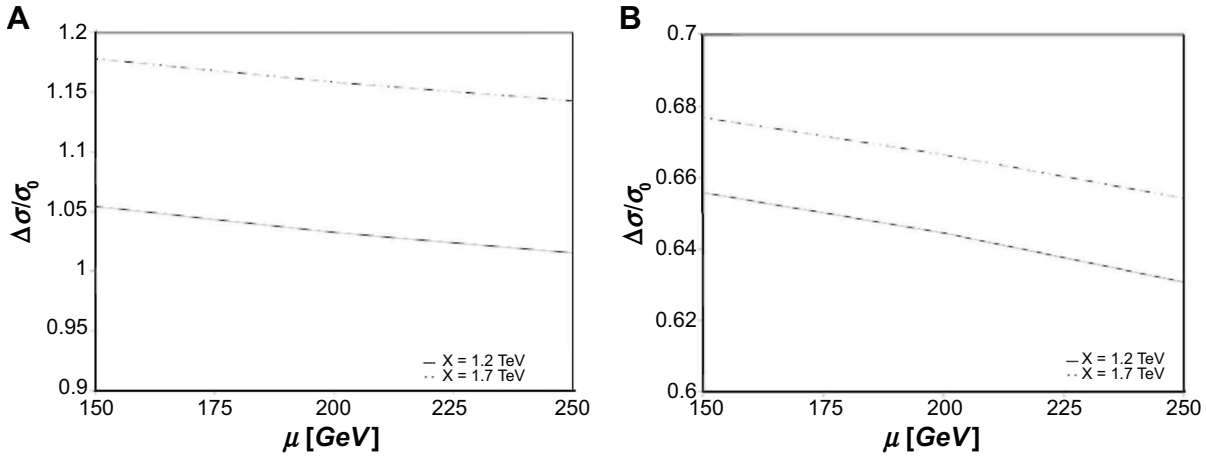

Figure 5. $\Delta\sigma/\sigma_0$ as a function of the supersymmetric Higgs mass parameter, μ.

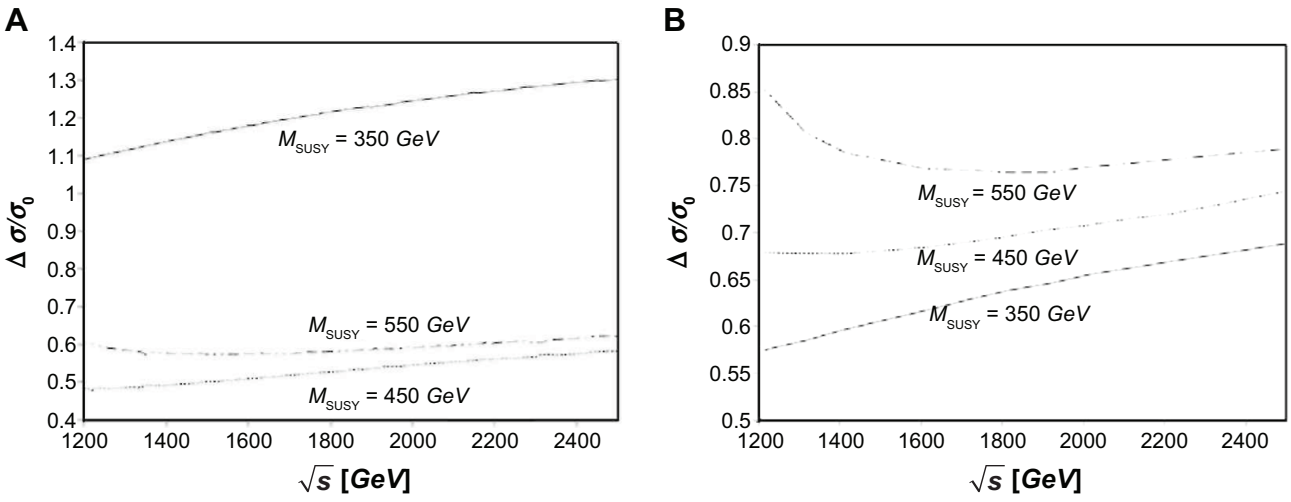

Figure 6. $\Delta\sigma/\sigma_0$ as a function of $\sqrt{s}$.

neutral Higgs particle mass, m_{h^0}, respectively. These plots are calculated from the change of the M_{SUSY} parameter of the $e^+e^- \rightarrow \tilde{\nu}_\tau \bar{\tilde{\nu}}_\tau h^0$ channel at the c.m.s energies 1, 1.5, and 2 TeV. These graphs show that σ_0 decreases with the increment of the tau-sneutrino mass, $m_{\tilde{\nu}_\tau}$, and the lightest neutral Higgs particle mass, m_{h^0}, respectively.

Figures 9 and 10 illustrate the influence of M_{SUSY} parameter on $m_{\tilde{\nu}_\tau}$ and m_{h^0}, respectively. These graphs clearly show that M_{SUSY} has a considerable impact on the tau-sneutrino and the lightest neutral Higgs particle masses of each of SPS 1b (Figs. 9A and 10A) and SPS 4 (Figs. 9B and 10B) scenarios, respectively.

3.2.3. Group III. Finally, we examine the impact of tan β parameter on the $\tilde{\nu}_\tau \bar{\tilde{\nu}}_\tau h^0$ production. The rest of the benchmark points of the mSUGRA model will remain as they are in Table 2.

Figure 11 exhibits the relationship between the percentage of the relative one-loop correction, $\Delta\sigma/\sigma_0$, and the colliding energy, $\sqrt{s}$, with μ = 250 GeV, for different values of tan β parameter.

Figures 12 and 13 show the impact of the tau-sneutrino mass, $m_{\tilde{\nu}_\tau}$, and the lightest neutral Higgs particle mass, m_{h^0}, which are calculated from the change in tan β parameter of the $e^+e^- \rightarrow \tilde{\nu}_\tau \bar{\tilde{\nu}}_\tau h^0$ process at the c.m.s energies 1, 1.5, and 2 TeV, respectively, of the tree-level cross-section σ_0. There is no significant effect in the value of σ_0 when m_{h^0} or $m_{\tilde{\nu}_\tau}$ is increased.

Figures 14 and 15 clarify the influence of tan β parameter on the tau-sneutrino and the lightest neutral Higgs particle masses ($m_{\tilde{\nu}_\tau}$ and m_{h^0}) at the tree level only. The minimal effect of tan β on the tau-sneutrino mass, $m_{\tilde{\nu}_\tau}$, is of order of 1 GeV. Its effect on the lightest neutral Higgs mass is considerable when its value is less than 8, but minimal when the value is above 8 for each of SPS 1b, (Fig. 15A) and SPS 4 (Fig. 15B) scenarios, respectively; this result is consistent with what we got in Ref.[12].

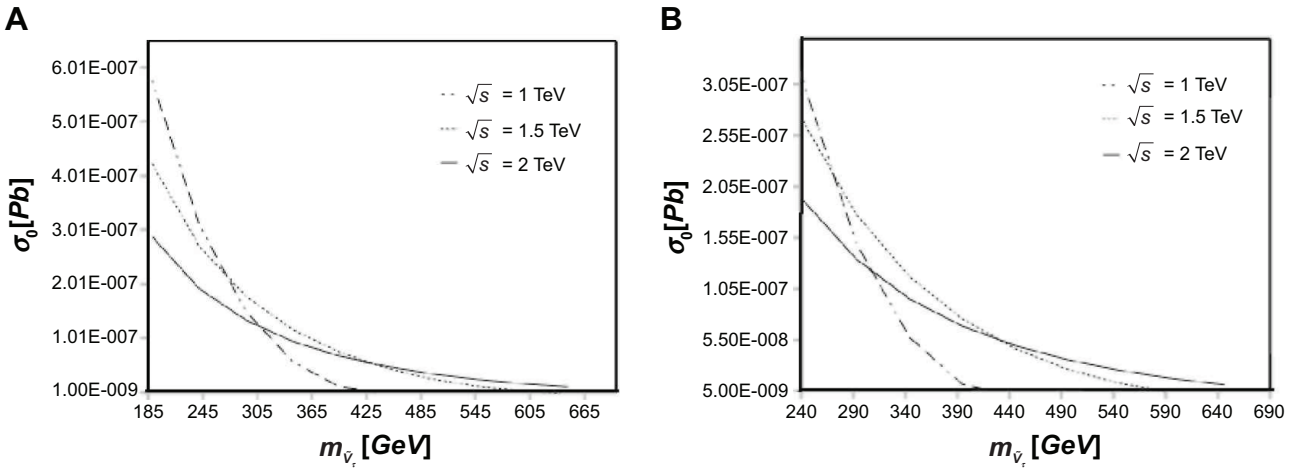

Figure 7. The dependence of σ_0 on $m_{\tilde{\nu}_\tau}$.

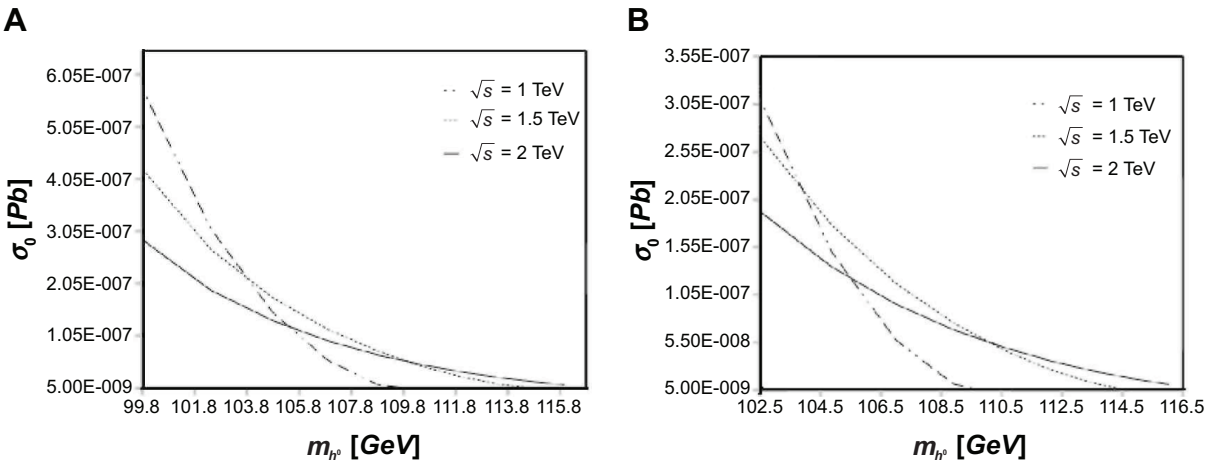

Figure 8. The dependence of σ_0 on m_{h^0}.

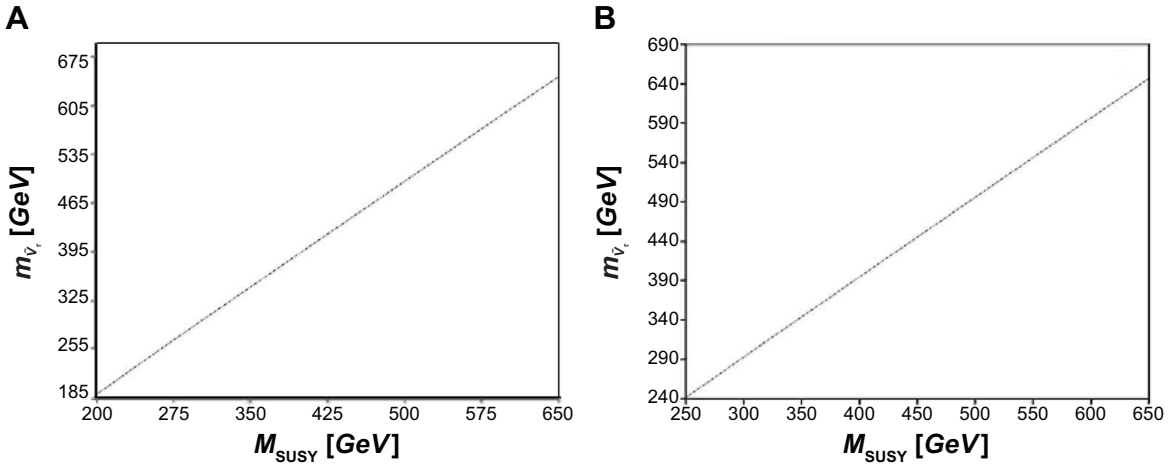

Figure 9. $m_{\tilde{\nu}_\tau}$ as a function of M_{SUSY} parameter.

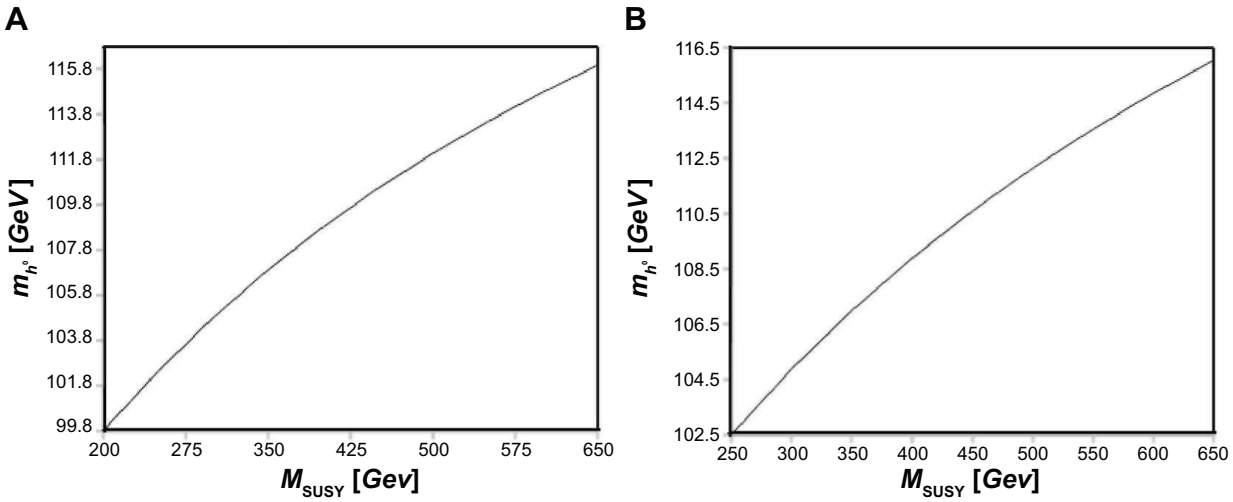

Figure 10. m_{h^0} as a function of M_{SUSY} parameter.

Table 5. Summary (Fig. 3): the maximum values of σ_0, σ, and σ_{QED} cross-sections of the SPS 1b and SPS 4 scenarios.

	$(\sigma_0)_{max}$/PB	$\sqrt{s}$/TeV	$(\sigma)_{max}$/Pb	$\sqrt{s}$/TeV	(σ_{QED})/Pb	
SPS 1b	5.77×10^{-7}	1	1.11×10^{-6}	1.1	1.83×10^{-8}	1.2
SPS 4	7.64×10^{-8}	1.6	1.26×10^{-7}	1.6	1.83×10^{-8}	1.2

Table 6. Summary (Fig. 4): the relationship between $\Delta\sigma/\sigma_0$ and $\sqrt{s}$ with $\mu = 250$ GeV.

	SPS 1B	SPS 4
	0.5 TeV → 2.5 TeV	1 TeV → 2.5 TeV
$\Delta\sigma/\sigma_0$	33% → 123%	63% → 71%

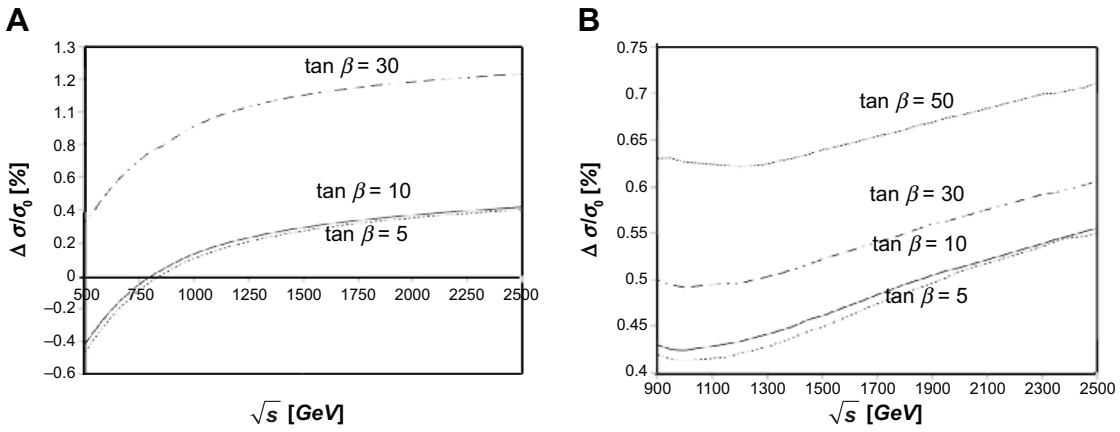

Figure 11. $\Delta\sigma/\sigma_0$ as a function of $\sqrt{s}$.

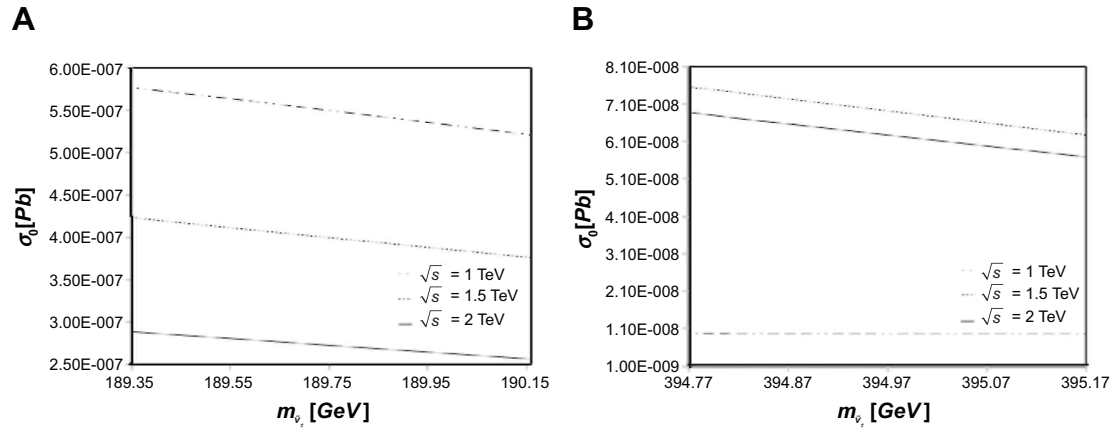

Figure 12. The dependence of σ_0 on the tau-sneutrino mass $m_{\tilde{\nu}_\tau}$.

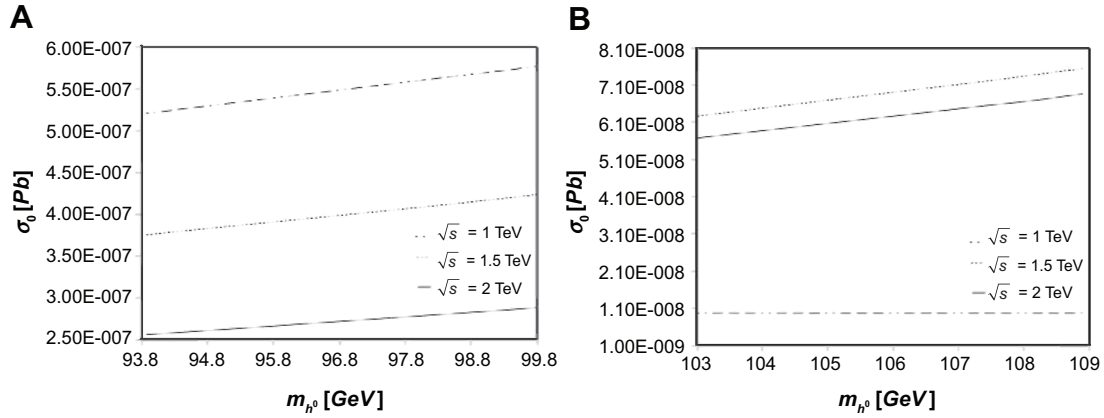

Figure 13. The dependence of σ_0 on the lightest Higgs mass m_{h^0}.

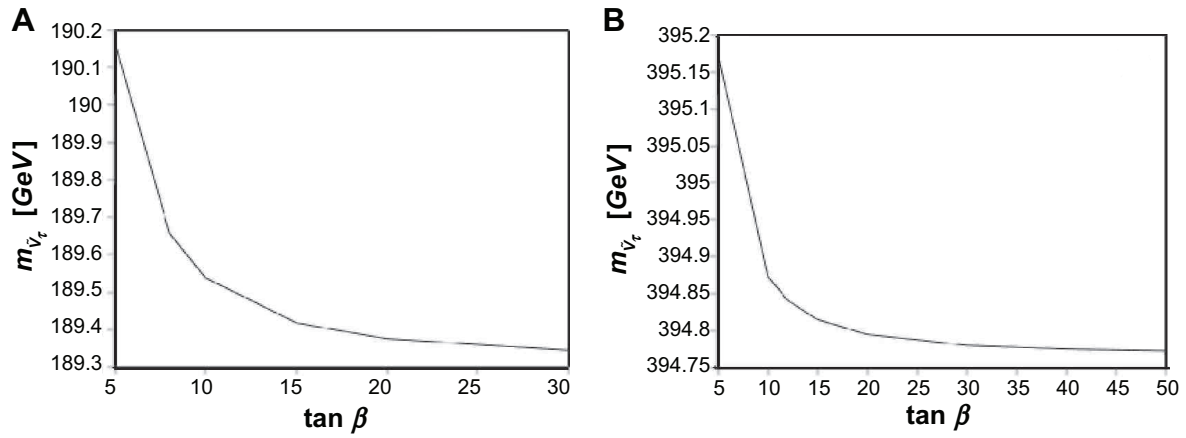

Figure 14. $m_{\tilde{\nu}_\tau}$ as a function of tan β parameter.

4. Conclusions

We have calculated with the help of FeynArts-3.6 and FormCalc-7.1 computer packages the Born cross-section and the full *EW* radiative correction as well as the soft-photon bremsstrahlung contribution for unpolarized beam to the $e^+e^- \to \tilde{\nu}_\tau \bar{\tilde{\nu}}_\tau h^0$ channel within the framework of the MSSM at linear collider (ILC). The hard-bremsstrahlung effects were not considered. One generally adopts the MSSM parameters at the two reference points SPS 1b and SPS 4 defined in the SPA project.

Our numerical results show clearly that the radiative corrections for the $e^+e^- \to \tilde{\nu}_\tau \bar{\tilde{\nu}}_\tau h^0$ channel for the two reference points SPS 1b and SPS 4 are always positive in our chosen parameter spaces. The relative correction varies in the range of [33%, 123%] as $\sqrt{s}$ goes from 0.5 to 2.5 TeV and of [63%, 71%] as $\sqrt{s}$ goes from 1 to 2.5 TeV for SPS 1b and SPS 4 benchmark points, respectively.

There is no significant impact of μ parameter on the total cross-section value at the Born approximation level or at the full virtual *EW*-corrected total cross-section for the two scenarios, SPS 1b and SPS 4.

The influence of the soft-breaking squark mass, M_{SUSY}, parameter on the tau-sneutrino and the lightest neutral Higgs particle masses at the tree level, σ_0, are considerable. A minimal effect ~1 GeV of the VEV, tan β, parameter on the tau-sneutrino mass, $m_{\tilde{\nu}_\tau}$, at the tree level, and on the lightest neutral Higgs particle mass, m_{h^0}, is considerable when tan β value is less than 8 for the two chosen parameter spaces.

The comparison between the two chosen parameter spaces shows that the cross-section values and the EW relative corrections for the $e^+e^- \to \tilde{\nu}_\tau \bar{\tilde{\nu}}_\tau h^0$ channel are in favor of the SPS 1b scenario, and these corrections are so remarkable and they that cannot be neglected if precise experimental analysis is sought.

Author Contributions

IAMA-M prepared all programs we needed to our numerical calculations. TAE-A designed the research plan and organised the study participated in all research. BYA-N carried out the numerical calculations, coordinated the data-analysis and contributed to the writing of the manuscript.

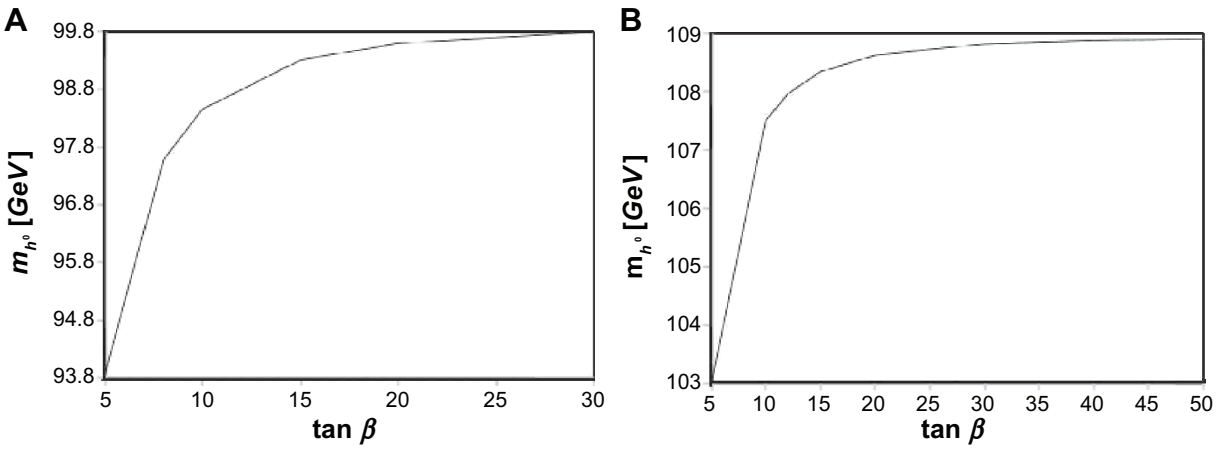

Figure 15. m_{h^0} as a function of tan β parameter.

Table 7. Summary (Fig. 5): the relationship between $\Delta\sigma/\sigma_0$ and the Higgsino mass parameter μ.

	$(\Delta\sigma/\sigma_0)_{max} \rightarrow (\Delta\sigma/\sigma_0)_{min}$	$(\Delta\sigma/\sigma_0)_{max} \rightarrow (\Delta\sigma/\sigma_0)_{min}$
	1.2 TeV	1.7 TeV
SPS 1b	105% → 102%	118% → 114%
SPS 4	66% → 63%	67.6% → 65.4%

REFERENCES

1. ALEPH, DELPHI, L3 and OPAL Collaborations The LEP Working Group for Higgs Boson Searches, Search for the Standard Model Higgs Boson at LEP. *Phys Lett B*. 2003:565. hep-ex/0306033.
2. Aaltonen T, Abazov VM, Abbott B, Abolins M, Acharya BS, Adams M, et al. The CDF, the D^0 Collaborations: Combination of Tevatron searches for the standard model Higgs boson in the W^+W^- decay mode. *Phys Rev Lett*. 2010;104: 061802. arXiv:1001.4162v3 [hep-ex].
3. Aad G, Abajyan T, Abbott B, Abdallah J, Abdel Khalek S, Abdelalim AA, et al. ATLAS Collaboration, Observation of a new particle in the search for the Standard Model Higgs boson with the ATLAS detector at the LH. *Phys Lett B*. 2012:716. arXiv: 1207.7214 [hep-ex] .
4. Ghosh S, Choudhury A, Sarma JK. Electromagnetic mass and charge of electrons at relativistic speed. *Indian J Phys*. 2013;87:607.
5. Nilles HP. Supersymmetry, supergravily and particle physics. *Phys Rept*. 1984;110:1. Haber HE, Kane GL. The search for supersymmetry: Probing physics beyond the standard model. *Phys Rept*. 1985;117:75. Barbieri R. Looking Beyond the Standard Model: The Supersymmetric Option. *Riv Nuovo Cim*. 1988;11N4:1.
6. Freitas A, von Manteuffel A, Zerwas PM. Slepton production at $e^+ e^-$ and e^-e^- linear colliders. *Eur Phys J C*. 2005;40:435. hep-ph/0408341.
7. Pandita PN, Patra M. Radiative Production of Lightest Neutralinos in e^+e^- collisions in Supersymmetric Grand Unified Models, *Int J Mod Phys A*. 2012:27. arXiv:1210.6477v1 [hep-ph].
8. Tsytrinov AV, Kalinowski J, Osland P, Pankov AA. Sneutrino identification in lepton pair production at ILC with polarized beams. *Phys Lett B*. 2012;718: 94–99. arXiv:1207.6234v1 [hep-ph].
9. Hebbeker T. Can the sneutrino be the lightest supersymmetric particle. *Phys Lett B*. 1999;470:259. arXiv:hep-ph/9910326v1.
10. Freitas A, Porod W, Zerwas PM. Determining Sneutrino Masses and Physical Implications. *Phys Rev D*. 2005;72:115002. arXiv:hep-ph/0509056v1.
11. Datta A, Djouadi A, Kneur J-L. Probing the SUSY Higgs boson couplings to scalar leptons at high-energy e^+e^- colliders. *Phys Lett B*. 2001;509:299–306. arXiv:hep-ph/0101353v1.
12. Al-Negashi BY, El-Azim TA, Abdul-Magead IAM. Neutral Higgs-boson production in association with a pair of muon-sneutrino at $e^+ e^-$ Linear Colliders. *IREPHY*. 2013;7: 3.
13. Mahmoud IS, El-Azim TA. Production of Lightest Neutral MSSM Higgs Boson in Association with s-Lepton Pairs at Electron Positron Colliders. *IREPHY*. 2012;6:6.
14. Allanach BC, Battaglia M, Blair GA, Carena M, De Roeck A, Dedes A, et al. The Snowmass Points and Slopes: Benchmarks for SUSY Searches. *Eur Phys J C*. 2002;25:113. arXiv:hep-ph/0202233v1.
15. Liu J-J, Ma W-G, Zhang R-Y, et al. Full one-loop electroweak corrections to h^0 (H^0, A^0) $H^\pm W^-$ productions at e^+e^- linear colliders. *Phys Rev D Part Fields*. 2007;75:053007. arXiv:hep-ph/0702156v2.
16. Denner A. Techniques for the calculation of electroweak radiative corrections at the one-loop level and results for W-physics at LEP200. *Fortschr Phys*. 1993;41:307. arXiv:0709.1075v1 [hep-ph].
17. Guasch J, Hollik W, Sola J. Fermionic decays of sfermions: a complete discussion at one-loop order. *J High Energy Phys*. 2002;10:040. arXiv:hep-ph/0207364v2; Hollik W, Kraus E, Roth M, Rupp C, Sibold K, Stöckinger D. Renormalization of the Minimal Supersymmetric Standard Model. *Nucl Phys B*. 2002;639:3–65. arXiv:hep-ph/0204350v2.
18. Hollik W, Rzehak H. The sfermion mass spectrum of the MSSM at the one-loop level. *Eur Phys J C*. 2003;32:127. arXiv:hep-ph/0305328v2.
19. Alwall J, Herquet M, Maltoni F, Mattelaer O, Stelzer T. MadGraph 5: Going Beyond. *J High Energy Phys*. 2011;06:128. arXiv: 1106.0522.
20. Giele WT, Glover EWN. Higher-order corrections to jet cross sections in $e^+ e^-$ annihilation. *Phys Rev D Part Fields*. 1992;46:1980–2010; Giele WT, Glover EW, Kosower DA. Higher Order Corrections to Jet Cross Sections in Hadron Colliders. *Nucl Phys B*. 1993;403:633. arXiv:hep-ph/9302225v1.
21. Beenakker W, Denner A, Dittmaier S, Mertig R, Sack T. High-energy approximation for on-shell W pair production. *Nucl Phys B*. 1993;410:245.
22. Hahn T. Generating Feynman Diagrams and Amplitudes with FeynArts 3. *Comput Phys Commun*. 2001;140:418. arXiv:hep-ph/0012260v2.
23. Agrawal S, Hahn T, Mirabella E. FormCalc 7. *J Phys Conf Ser*. 2012;368:012054. arXiv:1112.0124v1 [hep-ph].
24. Hahn T. Automatic Loop Calculations with FeynArts, FormCalc, and LoopTools. *Nucl Phys Proc Suppl*. 2000;89:231. arXiv:hep-ph/0005029v1; van Oldenborgh GJ, Vermaseren JAM. New Algorithms for One Loop Integrals. *Z Phys C*. 1990;46:425.
25. Beringer J, et al. (Particle Data Group), Review of Particle Physics. *Phys Rev D Part Fields*. 2012;86:010001.
26. Kovarik K, Weber C, Eberl H, Majerotto W. Complete one--loop corrections to $e^+ e^- > s_{f,i}\, s_{f,j}$. *Phys Lett B*. 2004;591:242–254. arXiv:hep-ph/0401092v2.
27. Heinemeyer S, Hollik W, Weiglein G. The Mass of the Lightest MSSM Higgs Boson: A Compact Analytical Expression at the Two-Loop Level. *Phys Lett B*. 1999;455:179. arXiv:hep-ph/9903404v1.
28. Aguilar Saavedra JA, Ali A, Allanach BC, Arnowitt R, Baer HA, Bagger JA, et al. Supersymmetry Parameter Analysis: SPA Convention and Project. *Eur Phys J C*. 2006;46:43. arXiv:hep-ph/0511344v2.
29. Allanach BC, Battaglia M, Blair GA, Carena M, De Roeck A, Dedes A, et al. The Snowmass Points and Slopes: Benchmarks for SUSY Searches. *Eur Phys J C*. 2002;25:1. arXiv:hep-ph/0202233v1.